

**SYNTHESIS OF POROUS CELLULOSE BEADS
INTERCALATED WITH CALCIUM CARBONATE
NANOPARTICLES FROM SODIUM
HYDROXIDE/UREA SOLUTION FOR DYE
ADSORPTION**

GAN WEI CHEE

UNIVERSITI SAINS MALAYSIA

2021

**SYNTHESIS OF POROUS CELLULOSE BEADS
INTERCALATED WITH CALCIUM CARBONATE
NANOPARTICLES FROM SODIUM
HYDROXIDE/UREA SOLUTION FOR DYE
ADSORPTION**

by

GAN WEI CHEE

**Project proposal submitted in partial fulfilment of the requirements for the
degree of Bachelor of Chemical Engineering**

2021

ACKNOWLEDGEMENT

First and foremost, I wish to express my indebted gratitude and special thanks to my project supervisor, Assoc. Prof. Ir. Dr. Leo Choe Peng, who has the substance of a genius: continually encouraged and guided me to be more professional. This paper would never have been completed without her assistance and dedicated participation in every phase of the process.

I would also extend my sincere appreciation to all the postgraduates, especially Miss Yap Jia Xin for their kind cooperation. They are not only sharing their ideas, valuable knowledge and skill but also willing to sacrifice their time in lending me a helping hand.

Furthermore, the physical and technical contribution of all the School of Chemical Engineering Universiti Sains Malaysia's academic and administrative staffs, laboratory technicians, especially Mrs. Yusnadia Mohd. Yusof is truly appreciated. Without their funding and support, this project could not have achieved its goal.

Apart from that, I would like to acknowledge the great love and support of my parents, Mr. Gan Lean Yuan and Mrs. Ooi Poh Lee and my siblings. In addition, I wish to express my deepest gratitude to my fellow friends and classmates, especially Mr. Lee Mun Yi. They kept me moving on and without their input, this work would not have been possible.

Once again, it is whole-heartedly appreciated to you all for the tremendous positive feedbacks given along with the continuous support received.

Gan Wei Chee

July 2021

TABLE OF CONTENTS

ACKNOWLEDGEMENT	i
TABLE OF CONTENTS	ii
LIST OF TABLES	iv
LIST OF FIGURES	v
LIST OF SYMBOLS	vii
LIST OF ABBREVIATIONS	viii
LIST OF APPENDICES	x
ABSTRAK	xi
ABSTRACT	xii
CHAPTER 1 INTRODUCTION	1
1.1 Background	1
1.2 Problem Statement	5
1.3 Research Objective.....	6
CHAPTER 2 LITERATURE REVIEW	7
2.1 Types of Adsorbent in the Removal of MB Dyes from Aqueous Phase.....	7
2.1.1 Activated Carbon (AC)	7
2.1.2 Clays.....	10
2.1.3 Alpha-Cellulose (α -Cellulose)	12
2.2 Cellulose Beads Preparation Strategies.....	16
2.2.1 Dissolution of Cellulose	20
2.2.1(a) Cellulose Dissolution with Chemical Reaction	21
2.2.1(b) Cellulose Dissolution without Chemical Reaction	22
2.2.2 Shaping Techniques into Spherical Particles	23
2.2.2(a) Dropping Techniques.....	23
2.2.2(b) Dispersion Techniques.....	25

2.2.3	Modification of Cellulose Beads.....	26
CHAPTER 3 METHODOLOGY.....		27
3.1	Materials.....	27
3.2	Preparation of PCBs intercalated with nano-sized CaCO ₃	29
3.3	Characterization of PCBs	30
3.4	PCBs Performance on adsorption of MB	31
3.5	Batch adsorption experiments	32
3.6	Adsorption kinetics	33
CHAPTER 4 RESULTS AND DISCUSSION.....		34
4.1	Chemical properties of PCBs samples	34
4.2	Morphology of PCBs samples.....	35
4.3	Adsorption kinetics of MB	38
4.3.1	Effect of adsorption dosage.....	38
4.3.2	Effect of equilibrium time	39
4.3.3	Effect of CaCO ₃ nanoparticles loading	40
4.3.4	Adsorption kinetics	42
4.3.5	Sustainability	46
CHAPTER 5 CONCLUSION.....		47
5.1	Conclusion.....	47
5.2	Recommendations	47
REFERENCES.....		48
APPENDICES		59

LIST OF TABLES

	Page
Table 1.1 Comparison between physisorption and chemisorption.	3
Table 2.1 Summary on adsorption capacities of MB dye using AC from different sources.....	9
Table 2.2 Summary on adsorption capacities of MB dye using clays.	11
Table 2.3 Summary on Q_e of MB dye using different modified cellulose.....	14
Table 2.4 Summary Table for the Cellulose Beads Preparation.	17
Table 3.1 Dilution table of preparing different MB concentrations using 100 ppm of MB as stock solution.	31
Table 4.1 MB adsorption using the various amount of CaCO_3 at equilibrium time (3 hr).....	41
Table 4.2 Kinetic model constant of the pseudo-first-order model and pseudo-second-order model for adsorption of MB onto PCBs.	44
Table 4.3 Kinetic parameters and correlation coefficient of the intraparticle diffusion model for adsorption of MB onto PCBs.	44

LIST OF FIGURES

	Page
Figure 1.1 Structure of cellulose.	4
Figure 2.1 Classification of cellulose solvent.	20
Figure 2.2 Schematic representation of dropping technology based on a vibrating nozzle (Mazzitelli et al., 2008).....	24
Figure 2.3 Cellulose beads preparation using dispersion technique (homogenizer) (Li et al., 2014).....	25
Figure 3.1 Flow diagram of the research project on PCBs intercalated with CaCO ₃	28
Figure 3.2 Experimental setup of the preparation of PCBs in CaCl ₂ solution.....	30
Figure 4.1 FTIR analysis of PCBs samples. (a) PCBs, (b) PCBs/0.01 wt% CaCO ₃ , (c) PCBs/0.03 wt% CaCO ₃ , (d) PCBs/0.05 wt% CaCO ₃	35
Figure 4.2 Cross-section morphology of PCBs samples at three different magnifications (×100, ×500, and ×1.0k). SEM images of (a,e,i) PCBs, (b,f,j) PCBs/0.01 wt% CaCO ₃ , (c,g,k) PCBs/0.03 wt% of CaCO ₃ , and (d,h,l) PCBs/0.05 wt% of CaCO ₃	37
Figure 4.3 Effect of adsorbent dosage on R and Q_e of MB at ambient pH and temperature.....	39
Figure 4.4 Effect of CaCO ₃ nanoparticles loading on Q_e of MB at ambient pH and temperature.....	40
Figure 4.5 Effect of CaCO ₃ nanoparticles loading on R of MB at ambient pH and temperature.....	41
Figure 4.6 PCBs samples (a) before and (b) after the dye removal.	42
Figure 4.7 Linear regression plots for the(a) pseudo-first-order kinetic model and (b) pseudo-second-order kinetic model.....	43

Figure 4.8 Intraparticle diffusion of MB dye on PCBs. 1 st phase refers to the time of 0 – 1.5 hr, 2 nd phase refers to the time of 1.5 – 3 hr, and 3 rd phase refers to the time of 3 – 5 hr.....	45
Figure 4.9 Life cycle of PCBs intercalated with CaCO ₃ nanoparticles.....	46
Figure 5.1 Modified syringe with with needle 0.88 mm in diameter.....	59
Figure 5.2 Calibration curve for absorbance against Ce.	59
Figure 5.3 Image of PCBs samples after adjusting color threshold, adding boundary in ImageJ.	60
Figure 5.4 Scale used to determine the particle sizes.....	60
Figure 5.5 Analyze particles with the range of size at 5.08 mm ² to infinity.....	61
Figure 5.6 Analyze particles with the range of size at 4.55 mm ² to 5.08 mm ²	61
Figure 5.7 Result for particle size of PCBs samples from ImageJ.....	62
Figure 5.8 Changes of dye solution for PCBs without additve of CaCO ₃ at the time of 0 hr to 5 hr.....	63
Figure 5.9 Changes of dye solution for PCBs with 0.01 wt% of CaCO ₃ at the time of 0 hr to 5 hr.....	63
Figure 5.10 Changes of dye solution for PCBs with 0.03 wt% of CaCO ₃ at the time of 0 hr to 5 hr.....	64
Figure 5.11 Changes of dye solution for PCBs with 0.05 wt% of CaCO ₃ at the time of 0 hr to 5 hr.....	64

LIST OF SYMBOLS

Symbol	Description	Unit
C_e	Equilibrium dye concentration of MB	mg/L
C_i	Adsorption constant	-
C_o	Initial dye concentration of MB	mg/L
k_1	Rate constant of pseudo-first-order kinetics	hr ⁻¹
k_2	Rate constant of pseudo-second-order kinetics	g/mg/hr
K_{di}	Intraparticle rate constant	g/mg/hr ^{1/2}
M	Weight of PCBs	mg
Q_e	Adsorption capacity	mg/g
Q_t	Adsorption capacity of MB at a given time	mg/g
S_{BET}	Specific surface area	m ² /g
t	Time of adsorption	hr
V	Volume of MB solution	L
R	Removal efficiency	%
R^2	Coefficient of determination for regression	-
λ_{max}	Maximum wavelength	nm

Greek Letter

α	Alpha
----------	-------

LIST OF ABBREVIATIONS

AC	Activated carbon
aq	Aqueous
ATR	Attenuated total reflectance
[BMIM]Cl	1-Butyl-3-methylimidazolium chloride
C	Carbon
CA	Cellulose acetate
CAC	Commercial activated carbon
CaCl ₂	Calcium chloride
CaCO ₃	Calcium carbonate
CO ₂	Carbon dioxide
CS ₂	carbon disulfide
CXA	Cellulose xanthate
DMSO/LiCl	Dimethylsulfoxide/Lithium chloride
DS	Degree of substitution
DTGS	Deuterated triglycine sulphate detector
Fe ₃ O ₄	Iron (III) oxide
FTIR	Fourier transform infrared
H	Hydrogen
HCl	Hydrochloric acid
H ₂ SO ₄	Sulphuric acid
HNO ₃	Nitric acid
HPAM/CNC	Hydrolyzed polyacrylamide/cellulose nanocrystal nanocomposite
ILs	Ionic liquids
LiBr	Lithium bromide
MB	Methylene blue
MCC	Microcrystalline cellulose
MCFBs	Magnetic cellulose/Fe ₃ O ₄ beads
NaOH	Sodium hydroxide
Na ₂ SO ₄	Sodium sulphate
NMMO	<i>N</i> -methylmorpholine <i>N</i> -oxide monohydrate
O	Oxygen

PDA	Polydopamine
PCBs	Porous cellulose beads
SAA	Succinic acid anhydride
SAB	Sodium alginate bipolymer
SEM	Scanning electron microscope
TiO ₂	Titanium dioxide
TMSC	Trimethylsilyl cellulose
UV-Vis	Ultraviolet-visible

LIST OF APPENDICES

- | | |
|------------|---|
| Appendix A | Modified syringe with a needle diameter of 0.8 mm |
| Appendix B | Calibration curve |
| Appendix C | Determination of particle sizes of PCBs through ImageJ Software |
| Appendix D | Dye solution before and after adsorption |

**SINTESIS MANIK SELULOSA BERPORI DISISIPKAN DENGAN
NANOPARTIKEL KALSIMUM KARBONAT DARI LARUTAN NATRIUM
HIDROKSIDA/UREA UNTUK PENJERAPAN PEWARNA**

ABSTRAK

Pewarna telah banyak digunakan dalam industri tekstil selama beberapa dekad terakhir dan industri tekstil menghasilkan 200,000 tan sisa pewarna setiap tahun. Dengan ini, proses penjerapan dengan penggunaan alfa-selulosa (α -selulosa) dipilih untuk menjerapkan pewarna dari air buangan kerana kelayakan ekonominya dan ketiadaan pencemaran sekunder. Walau bagaimanapun, kesan struktur supramolekul α -selulosa ini kurang dapat dijangkau oleh reagen. Oleh itu, tujuan kajian ini adalah untuk mensintesis dan mencirikan manik selulosa berliang (PCBs) untuk penyingkiran pewarna metilena biru (MB), dan menyiasat kesan nanopartikel kalsium karbonat (CaCO_3) disisipkan dengan sifat PCBs. Dalam kajian ini, PCBs dengan pelbagai jumlah nanopartikel CaCO_3 (0.01% bt, 0.03% bt dan 0.05% bt) sebagai penjerap berasaskan hijau berjaya dibuat. Apabila peningkatan ke 0.05% bt nanopartikel CaCO_3 pada PCBs, peningkatan kecekapan penyingkiran maksimum (R) MB dari 88.12% menjadi 97.04% pada dos penjerap 0.06 g dan masa keseimbangan 3 jam. Data eksperimen kajian kinetik penjerapan menggunakan sampel PCBs mengikuti model kinetic tertib pseudo-kedua, dengan nilai R^2 lebih tinggi dari 0.99, menunjukkan bahawa proses penjerapan diatur oleh pengerapan kimia. Kapasiti penjerapan maksimum PCBs dengan 0.05% bt muatan nanopartikel CaCO_3 ditentukan oleh urutan pseudo-detik ialah 4.91 mg/g. Hasilnya, penemuan kajian ini menghasilkan kaedah yang mudah dan berkesan untuk menghasilkan PCBs dengan nanopartikel CaCO_3 .

**SYNTHESIS OF POROUS CELLULOSE BEADS INTERCALATED
WITH CALCIUM CARBONATE NANOPARTICLES FROM SODIUM
HYDROXIDE/UREA SOLUTION FOR DYE ADSORPTION**

ABSTRACT

Dyes have become widely used in the textile industry over the last few decades and generates 200,000 tonnes of dye waste annually. Considering the situation, the adsorption process by using biodegradable alpha-cellulose (α -cellulose) is chosen for removing dye from wastewater due to its economic feasibility and absence of secondary pollution. However, a low degree of substitution occurs since this effect of α -cellulose's supramolecular structure is less reachable to reagents. Thus, the goals of this study are to synthesise and characterise porous cellulose beads (PCBs) for methylene blue (MB) dye removal, and to study the effects of calcium carbonates (CaCO_3) nanoparticles incorporated on PCBs properties and MB dye removal. In this study, PCBs with various amounts of CaCO_3 nanoparticles (0.01 wt%, 0.03 wt% and 0.05wt%) as green-based adsorbents were successfully fabricated. When the incorporation of 0.05 wt% of CaCO_3 nanoparticles on PCBs, the increment of maximum removal efficiency (R) of MB from 88.12% to 97.04% at the adsorbent dosage of 0.06 g and equilibrium time of 3 hr. The experimental data of adsorption kinetic studies on MB using PCBs samples were imitated by pseudo-second-order, with R^2 values of higher than 0.99, demonstrating that the adsorption process is governed by chemisorption. The maximum adsorption capacity of PCBs with 0.05 wt% of CaCO_3 nanoparticles loading determined by pseudo-second-order was 4.91 mg/g. As a result, the findings of this study resulted in a simple and effective method for producing PCBs with CaCO_3 nanoparticles loading.

CHAPTER 1

INTRODUCTION

Chapter 1 discusses the overview of this research and the importance of PCBs intercalated with CaCO_3 nanoparticles from NaOH/urea solution for dye removal. Generally, this chapter summarizes the significance of CaCO_3 and NaOH/urea aqueous solution in PCBs for removing dye, the problem statement and the research objectives of this research.

1.1 Background

Over the past decades, dyes are widely used in many industries, with the textile industry as the largest consumer (Li et al., 2020). Concerning this, 200,000 tonnes of dye waste are produced annually in textile industries (Ng & Leo, 2019). The removal of dyes from wastewater without proper treatment has raised significant concerns worldwide because dyes may lead to severe risks to the ecosystem and human health (Li et al., 2020; Li et al., 2019). The wastewater from domestic and industrial activities comprises both organic and inorganic pollutants (Liu et al., 2015). The textile industries produce wastewater containing dyes that are difficult to be removed using the common wastewater treatment systems. Textile dyes like MB will permanently injure humans and animals' eyes. MB also causes difficulty in breathing on inhalation, whereas ingestion through the mouth will cause vomiting, mental confusion and painful micturition. Thus, removing this colour effluent is environmentally important. However, dye removal is difficult due to its resistance to biodegradation (Kono 2015). Many technologies are available to remove dye from wastewater. Conventionally, biological treatment emerged as the most economical, effective and environmentally friendly technique. Unfortunately, this treatment is time-consuming, and it is not suitable for textile effluent since textile effluent is recalcitrant to biodegradation

(Mohan et al., 2007; Wawrzkievicz, 2012). Another technology that is available for dye removal is membrane separation, especially nanofiltration. Although membrane separation can remove common dyes, fouling of membrane and the high periodic replacement cost rank nanofiltration to be techno-economical inefficient (Wawrzkievicz, 2012; Sivarajasekar & Baskar, 2015). In view of the prevailing condition, the adsorption process has been chosen for removing dye from wastewater due to economic feasibility, high efficiency and less secondary pollution (Li et al., 2020; Li et al., 2019; Liu et al., 2015).

Adsorption is the process of purification or bulk separation, based on the concentration of the adsorbed components in the feed (Seader et al., 2010). The term adsorption indicates the accumulation at the interface of two phases of solute molecules, which including gas-solid interface or liquid-solid interface. The adsorbent is solid on which adsorption occurs and the adsorbate is the solute molecules that accumulate at the interface (Dabrowski, 2001). There are two principal modes of adsorption of molecules on surfaces; physisorption and chemisorption. Physisorption is involved weak Van der Waals forces between adsorbent and adsorbate and therefore the process is reversible in most cases (Seader et al., 2010). The formation of strong chemical or ionic bonds between molecules or adsorbate ions on the adsorbent surface is demonstrated by chemisorption, which is generally due to the exchange of electrons and hence it is an irreversible process (Seader et al., 2010). Most of the adsorbent depends on the physisorption and the key physical forces governing adsorption are hydrogen bonds, Van der Waals forces, and electrostatic forces. This process emerged as the alternative for curtail water contamination, especially if the cost of adsorbent is low and pre-treatment is not required (Dabrowski, 2001). Adsorption processes are widely applied to remove the chemical contaminants from waters for environmental

remediation purposes. The chemical contaminants mentioned before are those not impacted by traditional biological wastewater treatment (Dabrowski, 2001). Many factors affect the adsorption efficiency like pH, temperature, adsorbent surface area, adsorbent particle size and so on (Seader et al., 2010; Dutta, 2007). The reverse of the adsorption process is known as desorption. Adsorption is favoured at a higher pressure and lower temperature whereas desorption is favoured at lower pressure and higher temperature (Dutta, 2007). **Table 1.1** shows the comparison between physisorption and chemisorption.

Table 1.1 Comparison between physisorption and chemisorption.

Adsorption mode	Physisorption	Chemisorption
Heat of adsorption	Low, usually in the range of 20 – 40 kJ/mol	High, usually in the range of 40 – 400 kJ/mol
Force of attraction	Van der Waal’s forces	Chemical bond forces
Temperature	Low temperature	High temperature
Process	Reversible	Irreversible
Specific	Not very specific	Highly specific
Layers formed	Multi-molecular layers	Monomolecular layers
Activation energy	Does not require activation energy	Required activation energy

Conventionally, activated carbon (AC) is used to adsorb dyes from wastewater, but the difficulty in regenerating the AC restricts it to be used (Kono, 2015). In light of this, bio-adsorbent has gained recognition because of their low cost and sustainability (Li, et al., 2020). Cellulose, a linear $\beta - 1,4 - glycosidically$ linked polyglucan biopolymer considered as an nearly inexhaustible polymeric raw material with unique structure and properties as shown in **Figure 1.1** (Klemm et al., 2005). It is one of the most widely available, cheapest, environmentally friendly renewable natural biopolymers globally (Li et al., 2019). Therefore, a great deal of coverage has

been gained by cellulose which is considered excellent functional material for dye removal.

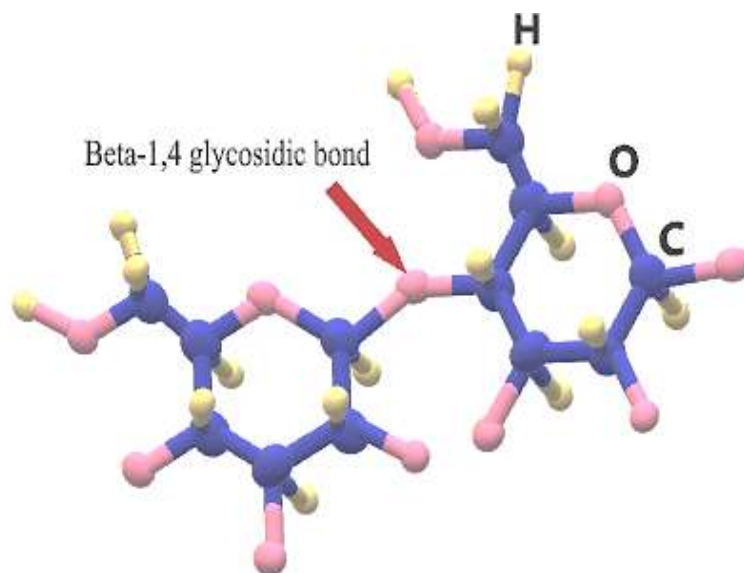


Figure 1.1 Structure of cellulose.

Nevertheless, it remains a challenge to dissolve cellulose in common solvents resulted from the strong intra- and inter-molecular hydrogen bonds. Aqueous NaOH/urea solution has been considered as a potentially promising green solvent due to the characteristics of low toxicity, nearly complete non-volatility, distinguished thermal stability and excellent dissolubility (Egal et al., 2008; Jin et al., 2007). When the aqueous solvents are cooled to roughly $-10\text{ }^{\circ}\text{C}$, they dissolve cellulose rapidly and provide clear solutions where the regeneration of cellulose may be occurred by coagulation in diluted acids (Gericke et al., 2013). Aqueous NaOH solutions are considered weak cellulose solvents in the viewpoint of thermodynamics. In respect of maximal concentration of cellulose and degree of polymerization, the dissolution process is rather restricted (Gericke et al., 2013). Nonetheless, usage of aqueous NaOH/urea solution for cellulose dissolution is suitable for the preparation of bead since the dropping method necessitates relatively low viscosities of the solution, for

example, low degree of polymerization and polymer concentration (Rosenberg et al., 2008; Sescousse et al., 2011; Luo & Zhang, 2009).

More recently, the development of nanocomposites based on cellulose devoted particular attention to enhancing the adsorption capacity of cellulose (Carla et al., 2010). CaCO_3 is an abundantly available biomineral as existed in both organisms and nature and has posed no toxic. Industrially, it has been used as the filler in plenty of composite materials by simply mechanically blended with another component (Carla et al., 2010). To increase the pore structure of PCBs, inorganic nanoparticles such as CaCO_3 can be added during the formation of PCBs (Li et al., 2020; Li et al., 2014). Considering this, the various size range of pores can be created through carbon dioxide (CO_2) released from the deposition of CaCO_3 (Li et al., 2020). Besides, full dispersion of PCBs and CaCO_3 is necessary to improve the properties of this nanocomposite (Tenhunen et al., 2018). The key factor in determining the structural uniformly and final physical performance of the system depends on the way to control the interactions between PCBs and CaCO_3 (Tenhunen et al., 2018).

1.2 Problem Statement

α -cellulose is a biodegradable and environmentally benign natural polymer generated by plants and trees. As α -cellulose molecules contain a large number of active hydroxyl groups, they may be readily chemically modified by introducing different functional groups on the hydroxyl (Yue et al., 2019). However, a low degree of substitution arises because the effect of the supramolecular structure of α -cellulose is less accessible by reagent (Liu et al., 2015; Klemm et al., 2005). The development of solvent systems such as NaOH/urea has been proposed to prepare cellulose

materials because some of these solvent systems are not practical as they are relatively high cost with limited reusability (Liu et al., 2015).

α -Cellulose is a commercial source that is readily available. Although it can be applied directly without further modification on the dye adsorption, its adsorption capacity is relatively low, which is only 4.95 mg/g (Tan et al., 2016). The low capacity of adsorption only relies on the weak electrostatic attraction between the α -cellulose surface in negatively charged and MB dye in positively charged. Therefore, modification of the pure α -cellulose is required to enhance this adsorbent's physical properties for dye removal. In this study, the porous cellulose in the form of beads will be incorporated with CaCO_3 as the secondary adsorbent. Therefore, the study of the addition of CaCO_3 is performed in the UV-Vis Spectrophotometer and the PCBs is characterized using scanning electron microscope (SEM), and Fourier transform infrared (FTIR).

1.3 Research Objective

- I. To synthesis and characterize PCBs for MB dye removal.
- II. To study the effects of CaCO_3 nanoparticles incorporated on PCBs properties and MB dye removal.

CHAPTER 2 LITERATURE REVIEW

Chapter 2 discusses the literature review of this thesis. The comparison of cellulose with other adsorbents for dye adsorption will be discussed in the first section. The following section will be discussed the method in the preparation of the cellulose beads is discussed in detail by reviewing the dissolution of cellulose in solvents, how to shape the solution into spherical particles and modification of cellulose beads.

2.1 Types of Adsorbent in the Removal of MB Dyes from Aqueous Phase

The adsorbent is a substance that adsorbs an adsorbate that has relatively high selectivity towards the adsorbent. Adsorbents are usually highly porous and allowing adsorption on the wall of the pores. Furthermore, different adsorbent performs different properties and it is important to select the suitable adsorbent in term of their adsorption capacity, porosity, pore size distribution and stability (Dutta, 2007). In the following sub-section, AC, clay and cellulose, which are applied as adsorbents for adsorption and removing dye from wastewater will be discussed.

2.1.1 Activated Carbon (AC)

AC is by far the most effective and commonly adsorbent used in dye removal from wastewater and the overview of Q_e using different AC is shown in **Table 2.1**. According to Kannan et al. (Kannan & Sundaram, 2001), the commercial AC (CAC) recorded a maximum Q_e of 980.3 mg/g as well as adsorption efficiency of 99.3% at pH 7.4 and 303 K. Despite its excellent performance, CAC remains an expensive material, thus various indigenously prepared AC can be used the low-cost alternative adsorbent materials. In the same report (Kannan & Sundaram, 2001), various indigenously prepared ACs used are straw AC (472.1 mg/g), rice husk AC (343.5

mg/g), coconut shell AC (277.9 mg/g), groundnut shell AC (164.9 mg/g) and bamboo dust AC (143.2 mg/g) and the results showed that under optimum experimental condition, they may be seen as low cost substitutes adsorbent to CAC. With intra-particle diffusion as one of the rate-determining steps, the adsorption method is found to be first order. In contrast to Kannan et al., Hameed et al. (Hameed et al., 2007) mentioned bamboo could be an effective adsorbent to removing MB dye from aqueous solution and its maximum Q_e (454.2 mg/g) is greater than the earlier studies due to porous structure of AC with wide internal surface area (1896 m²/g).

The Q_e of jute fiber carbon was 225.64 mg/g at pH 4 and 301 K based on Senthilkumaar et al. (Senthilkumaar et al., 2005). However, the optimum pH was to be in the range of 5-10 as the decreasing of surface charge density with increasing the pH solution. Subsequently, the electrostatic repulsion between the surface of the carbon and the positively charged MB dye is lowered, thereby increasing the rate of adsorption. Furthermore, the use of agricultural solid wastes like raw olive stone (16.12 mg/g) (Hazzaa & Hussein, 2015) and apricot stones (36.68 mg/g) (Dijilani et al., 2015) were also an alternative for the removal of MB and followed the adsorption kinetic model with pseudo-second-order. The introduction of oxygenated groups onto the surface of the AC during chemical activation enhances the adsorption process (Dijilani et al., 2015). AC produced from fuel oil residues is also a potential low-cost dye removal material from downstream (Jarrah, 2017). El Qada et al. (2008) reported the AC produced by steam activation and it was noticed that AC produced from New Zealand coal (588 mg/g) resulted in the greatest adsorption capacity of MB dye, continued with AC produced from Venezuelan bituminous coal (380 mg/g) at pH 11 and 293 K. A decrease in particle size of adsorbent lead to increase the adsorption capacity, but adsorption maybe restricted to its external surface area.

Table 2.1 Summary on adsorption capacities of MB dye using AC from different sources.

Adsorbent	S_{BET} (m ² /g) ^e	Size ^f	Maximum Q_e (mg/g)	R (%)	Ref.
CAC	-	0.09 mm	980.30	99.3	(Kannan & Sundaram, 2001)
Straw AC	-	0.09 mm	472.10	98.9	(Kannan & Sundaram, 2001)
Coconut shell AC	-	0.09 mm	277.90	93.7	(Kannan & Sundaram, 2001)
Rice husk AC	-	0.09 mm	343.50	97.9	(Kannan & Sundaram, 2001)
Groundnut shell AC	-	0.09 mm	164.90	94.2	(Kannan & Sundaram, 2001)
Bamboo dust AC	-	0.09 mm	143.20	93.9	(Kannan & Sundaram, 2001)
Jute fiber carbon	-	0.42 mm	225.64	-	(Senthilkumaar, et al., 2005)
Bamboo based AC	1896.0	1.00-2.00 mm 2.34 nm	454.2	-	(Hameed et al., 2007)
Olive stones AC	-	0.40-0.80 mm	16.12	94.0	(Hazzaa & Hussein, 2015)
Apricot stones AC	359.4	0.15-0.25 mm	36.68	99.0	(Dijilani et al., 2015)
AC from fuel oil	50.7	17.18 nm	85.60	-	(Jarrah, 2017)
AC (New Zealand coal)	857.14	1.21 nm	588.00	99.8	(El Qada et al., 2008)
AC (Venezuelan nituminous coal)	863.5	< 0.11 mm 1.23 nm	380.00	-	(El Qada et al., 2008)

^e S_{BET} : Specific surface area; ^f Value in mm : bead size; Value in nm : pore size.

2.1.2 Clays

Since the CAC is being a limited natural resource, with high cost and difficulty of regeneration, clay derivatives become important in dye adsorption for wastewater treatment. Clay minerals do not only have strong sorption and complexation ability but also low cost, thus they have been extensively studied recently. A deeper understanding of MB adsorption capacity onto functionalized sodium alginate biopolymer (SAB) beads with λ -carrageenan-calcium phosphate, celite 545 and carboxylated cellulose had been reported by Jabli et al. (Jabli et al., 2020). Q_e of the mentioned alginate composites followed the order: SAB with celite 545 (7.5 mg/g) > SAB with λ -carrageenan-calcium phosphate (6.8 mg/g) > SAB with carboxymethyl cellulose (6.5 mg/g) (Jabli, et al., 2020). This trend can be explained by the weakening of adsorptive forces between the cationic dye molecules and the reactive groups of the prepared adsorbent, indicating exothermic mode controlled the MB adsorption.

Oussalah et. al. (2019) reported a hybrid alginate/natural bentonite composite beads, which in low in cost, with the ratio of alginate to bentonite equal to 1 to 1 (A-B 1/1) displaying the maximum Q_e toward MB of 1213 mg/g and the specific surface area (S_{BET}) of 11.04 m²/g. The highest adsorbed amount of MB through A-B 1/1 adsorbents can be due to the strong interaction between the cationic charge of dye and the carboxylate group of alginate, at the same time, they can be regenerated (Oussalah et al., 2019). According to Othman et al. (2020), alginate with AC/copper ferrite with porous rough structure (S_{BET} of 31.43 m²/g; average pore diameter of 5.66 nm) emerged as a promising material to adsorb dyes from wastewater since the results revealed the maximum Q_e of 400.0 mg/g for MB. Other than alginates, chitosan-clay bio-composite beads act as the potential adsorbent in removing MB dye from the real effluent and showing R of MB dye of 50.90% (Biswas et al., 2020). The better

performance from the MB uptake when the biocomposite was rich in clay as compared to chitosan. **Table 2.2** shows the overview of the adsorption capacities of MB dye using clays.

Table 2.2 Summary on adsorption capacities of MB dye using clays.

Adsorbent	S_{BET} (m ² /g)	Size ^g	Maximum Q_e (mg/g)	R (%)	Ref.
SAB with carboxymethyl cellulose	-	-	6.500	-	(Jabli et al., 2020)
SAB with λ -carrageenan-calcium phosphate	-	-	6.800	-	(Jabli et al., 2020)
SAB with celite 545	-	-	7.500	-	(Jabli et al., 2020)
Hybrid alginate(A)/natural bentonite(B) composite beads (A-B 1/1)	11.04	< 0.10 mm	1213.000	99.65	(Oussalah et al., 2019)
Alginate with activated carbon/copper ferrite	31.43	4.00 nm 5.66 nm	400.000	98.00	(Othman et al., 2020)
Chitosan-clay biocomposite beads	-	-	2.385	40.60 ^h	(Biswas et al., 2020)

^g Value in mm : bead size; Value in nm : pore size. ^hFor specific species removal from standard aqueous solution at non-optimized conditions.

2.1.3 Alpha-Cellulose (α -Cellulose)

Numerous methods like biological, chemical, physical, and combined processes were utilized in extracting cellulose from plants (Tan et al., 2016; Li et al., 2020). According to Tan et al. (2016), the study of the adsorption mechanism of MB dye onto native cellulose was carried out and the electrostatic attraction between the negatively charged cellulose surface and positively charged MB dye was observed as the key adsorption mechanism. Subsequently, the quick adsorption of the MB dye was stated and proved that cellulose is a promising green adsorbent although was threatened by low Q_e (4.95 mg/g) (Tan et al., 2016). In another approach, immobilization of cellulose isolated from oil palm fronds showed the Q_e up to a maximum of 12.85 mg/g and indicated the improvement from pure cellulose (Tan et al., 2018). When water was presented, the fibres will swell and followed by expansion of pore fibres (1.29 nm). Consequently, the hydrogen linkages formed with the molecules of dye is promoted (Tan et al., 2018). In another development, isolation of microcrystalline cellulose (MCC) from oil palm fronds through acid hydrolysis possesses excellent properties to adsorb MB dye, resulting in a monolayer adsorption capacity up to 51.81 mg/g (Hussin et al., 2016). Based on Zhou et al. (2014), the improvement of maximum dye adsorption capacity of partially hydrolyzed polyacrylamide/cellulose nanocrystal nanocomposite (HPAM/CNC) hydrogel at the low swelling ratio. Li et al. (2020) discovered the maximum adsorption of MB dye by porous magnetic cellulose/Fe₃O₄ beads (MCFBs) to be 1186.8 mg/g at the operating condition of pH 7 and 318 K. This is due to the well-dispersed of Fe₃O₄ particles rendered MCFBs magnetic. Therefore, MCFBs are magnetically separable and result in a variety of green-based adsorbents with easy recovery.

To further enhance the adsorption performance of cellulose, maleic anhydride-modified cellulose beads were formed by dissolving and regenerating in the existence of maleic anhydride and its maximum monolayer capacities for MB was obtained at 117.65 mg/g (Li, et al., 2014) and 194.6 mg/g (Zhou et al., 2012). On the other hand, the carboxylated cellulose beads with high porosity exhibited a remarkable adsorption capacity of 281.81 mg/g (Meng et al., 2019), which is approximately 8 times more than unmodified porous cellulose microbeads with Q_e of nearly 49.0 mg/g (Hua et al., 2019). Concerning this, more open-pores is sometimes found on the carboxylated cellulose beads compared to pure cellulose microbead and the S_{BET} was increased from 99.80 m²/g of pure cellulose microbead to 156.86 m²/g of carboxylated cellulose bead. A simple process for the production of bio-inspired MCC hydrogel functionalized by polydopamine (PDA) coating, which was achieved by self-polymerization of dopamine in the MCC/lithium bromide (LiBr) solution (Sun et al., 2016; Wei et al., 2018). As a result, this new kind of aerogels displayed superior adsorption efficiency and high adsorption capacity against MB. He et al. (He et al., 2013) studied the carboxylated nanocrystalline cellulose through hydrolysis of MCC in ammonium persulfate with a maximum Q_e of 101.16 mg/g. Overall, the adsorption efficiency of the different MCC adsorbents is more than 75% at operating conditions of pH 7-9 and under room temperature. **Table 2.3** shows the overview of Q_e of MB dye using MCC from different techniques.

Table 2.3 Summary on Q_e of MB dye using different modified cellulose.

Adsorbent	S_{BET} (m ² /g)	Size/ Morphology ^{i,j}	Maximum Q_e (mg/g) ^j	R (%)	Ref.
Cellulose	1.32	0.05 mm	4.95	> 85.00	(Tan et al., 2016)
MCC from oil palm frond	5.64	1.97 nm	51.81	-	(Hussin et al., 2016)
Immobilized cellulose	9.47	1.29 nm	12.85	76.39	(Tan et al., 2018)
HPAM/CNC hydrogel	-	350.50 g/g (P30C10-6.5)	170.56 (P30C10-6.5)	90.00	(Zhou et al., 2014)
		269.50 g/g (P30C20-6.5)	244.80 (P30C20-6.5)		
		73.10 g/g (P30C20-5.0)	326.08 (P30C20-5.0)		
MCFBs	8.23	~2.50 mm	1186.80	88.40	(Li et al., 2020)
Maleic anhydride- modified cellulose beads	0.73	< 0.05 mm	117.65	97.11	(Li et al., 2014)
Cellulose modified with maleic anhydride	-	68.14 %	194.60	97.86	(Zhou et al., 2012)

Table 2.3 (Continued)

Adsorbent	S_{BET} (m ² /g)	Size/ Morphology ^{i,j}	Maximum Q_e (mg/g) ^j	R(%)	Ref.
Carboxylated cellulose beads	156.86	2.08 mm	288.81	87.99	(Meng et al., 2019)
Porous cellulose microbeads	99.80	2.40 mm	48.80	90.00	(Hua et al., 2019)
MCC with pyridone derivatives	-	2.88 mmol/g	142.86(PDA-SAA-MCC)	87.00	(Sun et al., 2016)
MCC/PDA aerogel	36.92	-	153.40	96.00	(Wei et al., 2018)
Carboxylated Nanocrystalline cellulose	367.00	6.54 nm	101.16	90.00	(He et al., 2013)

ⁱ Value in mm : bead size; Value in nm : pore size; Value in g/g : swelling ratio; Value in % : degree of crystallinity; Value in mmol/g : bonded amount ^j P30C10-6.5 : 30 wt% of HPAM & 10 wt% of CNC at pH 6.5; P30C10-6.5 : 30 wt% of HPAM & 20 wt% of CNC at pH 6.5; P30C20-5.0 : 30 wt% of HPAM & 20 wt% of CNC at pH 5.0; PDA : Polydopamine; SAA : Succinic acid anhydride.

2.2 Cellulose Beads Preparation Strategies

The synthesis of spherical cellulose beads by transferring a viscose solution into a coagulation bath in an aqueous form by using a dropper was firstly introduced in the US patent (O'Neill & Reichardt, 1951). Since then, much attention has been paid to obtaining the various size of cellulose beads by using different solvents and techniques as shown in **Table 2.4**. The two simplified steps for cellulose beads production are firstly dissolution of cellulose in solvents, followed by shaping into spherical particles and solidify the solution particles to their desired size (Li et al., 2020). Subsequently, the adsorption capacity of cellulose beads could be improved by modifying cellulose beads. The points mentioned above were discussed in detail separately to obtain a systematic overview.

Table 2.4 Summary Table for the Cellulose Beads Preparation.

Shaping technique	Starting material ^a	Type of Solvent ^b	Solidification ^c	Modification ^d	Bead size (mm)	Ref.
Dropping	Cellulose	[BMIM]Cl	Solidification at -10 °C, washing with water/ethanol	1. Addition of CaCO ₃ , 2. Surface grafting	~3.0	(Li et al., 2020)
		DMA/LiCl	Coagulation in water/alcohol	-	~0.5	(De Oliveira & Glasser, 1996)
		NMMO	Coagulation at 10 °C, washing with water	-	~2.0	(Niemz & Vorbach, 2002)
		NMMO	Coagulation in water	Addition of chitosan	-	(Twu et al., 2003)
		NaOH/urea _{aq}	Coagulation in HNO _{3aq}	-	~ 2.0	(Trygg et al., 2013)

Table 2.4 (Continued)

Shaping technique	Starting material ^a	Solvent ^b	Solidification ^c	Modification ^d	Bead size (mm)	Ref.
Dropping	Cellulose	NaOH _{aq}	Coagulation in water	Addition of Fe ₂ O ₃ -nanoparticles, active carbon	~ 2.0	(Luo & Zhang, 2009)
		NaOH _{aq}	Coagulation in H ₂ SO _{4aq}	-	~0.5	(Rosenberg et al., 2008)
		NaOH/urea _{aq}	Coagulation in H ₂ SO ₄ and Na ₂ SO ₄	Addition of CaCO ₃	2.0	(Hua et al., 2019)
		NaOH/urea _{aq}	Coagulation in H ₂ SO ₄ and Na ₂ SO ₄	1. Addition of CaCO ₃ 2. Carboxylation	~3.0	(Meng et al., 2019)
	CA	Acetone/DMSO	Coagulation in water, saponification with NaOH _{aq}	-	~1.0	(Chen & Tsao, 1976)
CXA	NaOH _{aq}	Coagulation in HCl _{aq}	Addition of CaCO ₃	~4.0	(Sakurai et al., 1997)	

Table 2.4 (continued)

Shaping technique	Starting material ^a	Solvent ^b	Solidification ^c	Modification ^d	Bead size (mm)	Ref.
Dispersion	Cellulose	Ionic liquids	Coagulation with ethanol	Addition of tungsten carbide	0.1-0.3	(Shi et al., 2010)
		NaOH _{aq}	Solidification at 90 °C, washing with water/ethanol/acetone	1. Addition of pyridine 2. Carboxylation	-	(Zhou et al., 2012)
	CXA	NaOH/ urea _{aq}	Coagulation in HCl _{aq} , washing with water/acetone	1. Addition of CaCO ₃ , alkaline-treated diatomite 2. Esterification	-	(Li et al., 2014)
		NaOH/ urea _{aq}	Coagulation in HCl _{aq}	Addition of Fe ₂ O ₃ -nanoparticles	~0.2	(Luo & Zhang, 2010)
	CXA	NMMO	Solidification at 10 °C, washing with water/alcohol	Addition of tungsten carbide	0.075-0.3	(Phottraithip et al., 2011)
		NaOH _{aq}	Solidification at 90 °C	1. Addition of CaCO ₃ 2. Cross-linking	~0.1	(Wang et al., 2007)
		NaOH _{aq}	Solidification at 90 °C	1. Addition of TiO ₂	-	(Lei et al., 2003)

^aCA : Cellulose acetate; CXA : Cellulose xanthate ^b DMSO/LiCl : Dimethylsulfoxide/Lithium chloride; NMMO : *N*-methylmorpholine *N*-oxide monohydrate; NaOH : Sodium hydroxide; aq : aqueous; [BMIM]Cl : 1-Butyl-3-methylimidazolium chloride ^c HNO₃ : Nitric acid; H₂SO₄ : Sulphuric acid; Na₂SO₄ : Sodium sulphate ^d Fe₂O₃ : Iron (III) oxide; CaCO₃ : Calcium carbonates; TiO₂ : Titanium dioxide; - : No available data

2.2.1 Dissolution of Cellulose

Cellulose has a strong crystalline structure as it formed a strong inter- and intramolecular hydrogen bonding network and consequently it is insoluble in organic solvents and water (Li et al., 2019; Liu et al., 2015; Gericke et al., 2013). Cellulose can only be dissolved if the inter- and intramolecular hydrogen bonds are effectively disrupted (Sen et al., 2013). Generally, two different categories of cellulose dissolution processes can be distinguished: (1) cellulose dissolution with chemical conversion and (2) cellulose dissolution without chemical conversion. For cellulose dissolution with chemical conversion, derivatizing cellulose solvents with isolation of the intermediate and without isolation will be addressed. For dissolution of cellulose without chemical conversion, non-derivatizing solvents are competent to dissolving cellulose by physical interactions without chemical modification. **Figure 2.1** shows the classification of solvent for cellulose dissolution.

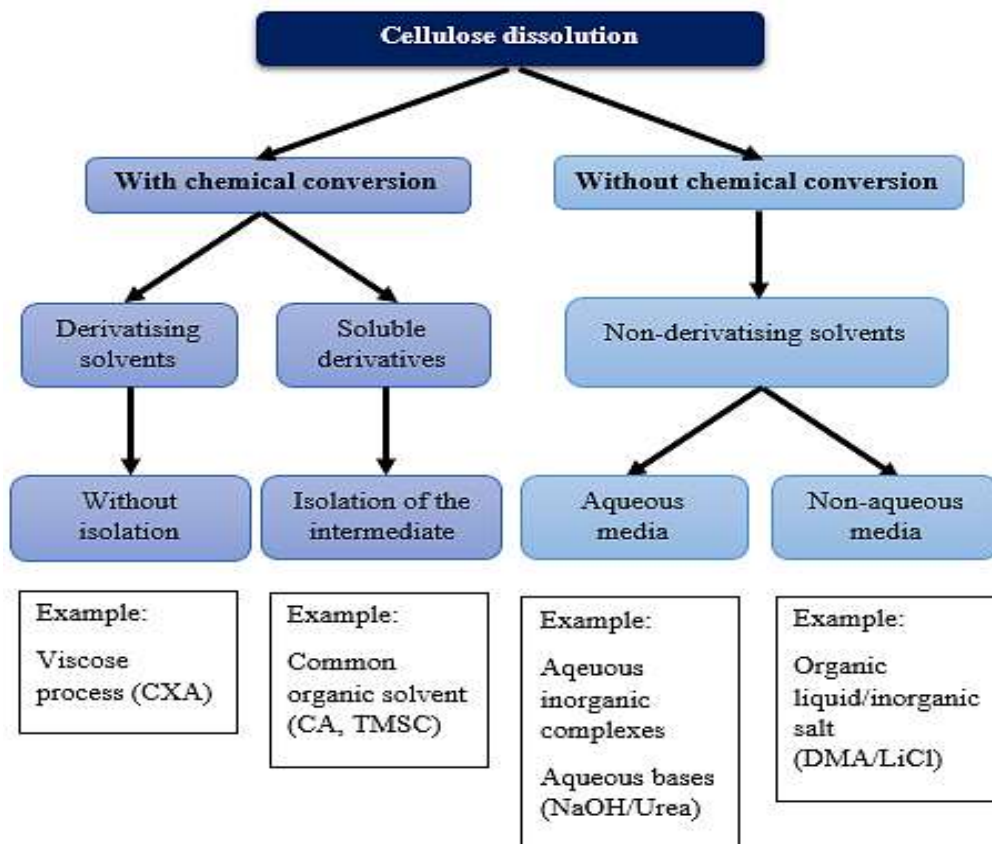


Figure 2.1 Classification of cellulose solvent.

2.2.1(a) Cellulose Dissolution with Chemical Reaction

The most important example of utilizing a derivatizing cellulose solvent is the viscose process. It was the most intensively researched method of dissolution in preparing cellulose beads after being employed by O'neill et. al. (O'Neill & Reichardt, 1951) for the first time when dropping the solution of cellulose xanthate (CXA) in a coagulation bath, which existed in an aqueous phase. Conversion of cellulose into CXA by a series of alkalization, ageing and carbon disulfide (CS_2). Subsequently, CXA is directly processed without isolation from the reaction mixture and the polysaccharide is replenished by cleaving the substituent of xanthate after the shape of the bead was obtained from the solution. The cleavage process can be achieved by increasing the temperature at 90 °C several times or by acid hydrolysis. Nevertheless, the highly toxic CS_2 is not environmentally friendly and makes it the major drawback of the viscose process. Therefore, ionic liquids (ILs) have been paying attention to by a lot of researchers recently as an environmentally friendly alternative.

Furthermore, cellulose acetate (CA) acts as a rather stable cellulose derivative is another commonly applied derivative to synthesis cellulose beads. Two important procedures make this solvent system differs from using derivatizing solvents. Firstly, isolation of CA is possible and can be kept after preparation, thus it is not necessary to process immediately. Secondly, during the regeneration process, acetyl moiety is not cleaved. Therefore, the extra step of processing is needed in converting cellulose derivative beads into cellulose beads, where CA is precipitated by using a non-solvent, like water to replace the inorganic solvent (Chen & Tsao, 1976). Different degrees of substitution (DS) can be used to form CA by either esterifying cellulose with an acetic acid chloride or anhydride in various heterogeneous or homogeneous systems (Wang et al., 2018). The key downside to procedures using cellulose derivative as a precursor

is the extra processing steps needed for the implementation and finally removal of acetyl moieties.

2.2.1(b) Cellulose Dissolution without Chemical Reaction

Procedures that involved derivatization and changed back into cellulose needed more energy and formed a high level of toxic waste. Concerning this, cellulose can be dissolved directly by using non-derivatizing solvents, without chemically modifying the polysaccharide, followed by coagulation in a non-solvent is the most effective procedure for synthesising cellulose beads. For decades, aqueous metal salt solutions like cuprammonium hydroxide, which contain coligands and it was among the first reported for cellulose dissolution by complexing of its hydroxyl groups. However, their application is currently highly limited due to the presence of heavy metals (Gericke et al., 2013). Dissolution of cellulose in N,N-dimethylacetamide (DMA) containing lithium chloride (LiCl) and under homogeneous conditions, cellulose has been extensively used for the chemical derivatization of the polysaccharide (De Oliveira & Glasser, 1996). Formation of cellulose and cellulose/polymer blends into fibres, films and materials with extremely porous can also be achieved by using this solvent. Although it is useful in terms of dissolution capacity and the ability to prepare to blend products, the high costs and limited recyclability of the DMA/LiCl make its little use for cellulose production outside academic study.

Furthermore, non-derivatizing cellulose solvent like N-methylmorpholine N-oxide (NMMO) normally acts as an alternative, which has been intensively studied to replacing CS₂ due to safety and environmental concerns. Cellulose beads can be formed through the creation of cellulose/NMMO droplets in a spherical shape, whether through dropping or dispersing methods, solidification by lowering temperatures, then by the elimination of NMMO residues from the preformed particles by rinsing with

water (Niemz & Vorbach, 2002; Twu et al., 2003; Phottraithip et al., 2011). Unwillingly, NMMO is thermally unstable, particularly as regards additional additives such as AC (Gericke et al., 2013). Recently, aqueous NaOH solutions combined with urea that avoid gelation gained much attention in this context as the ingredients are cheap, non-toxic and environmentally friendly (Li et al., 2014; Hua et al., 2019; Xie et al., 2019; Rosenberg et al., 2008). The aqueous solvents rapidly dissolve cellulose upon cooling to around -10 °C, thereby create transparent solutions from which regenerated the cellulose and used diluted acids to coagulate it (Wang et al., 2012). These aqueous solutions are suitable for bead preparation due to its shaping step requires relatively low solution viscosities. Also, improvement of the solubility of cellulose can be developed by efficient pretreatment, in particular via dropping techniques or dispersion techniques (Gericke et al., 2013).

2.2.2 Shaping Techniques into Spherical Particles

The molding of the beads from a solution of polysaccharides will either be obtained by dropping or dispersing techniques. Apart from the technological aspects, this separation is also a macroscopic separation into bead-shaped cellulose with a scale of more than 250-500 µm through dropping procedures and below 250-500 µm through dispersion procedures.

2.2.2(a) Dropping Techniques

Dropping techniques involved the creation and solidification (in a coagulation bath containing non-solvent) of spherical droplets of a polysaccharide solution. A droplet is formed by pressing fluids through the thin hole such as the syringe nozzle as shown in **Figure 2.2**. This is due to the combination of the pressure and gravitational forces applied for ejection reaches a certain value that can be measured by capillary forces at the outlet and solution's surface tension. The vibration of nozzles, which are

targeted at the capillary tip from where the solution protrudes, forced the formation of smaller droplets (Mazzitelli et al., 2008). This technique has limited the diameter of cellulose beads to a maximum of approximately 0.5 to 3 mm. The length to the width factor is dependent on the mechanical pressure that the droplets experience as they reach the coagulation bath's surface. Flattening of the beads might happen and result in a disk-like shape due to the higher force applied than the stability of droplets. Consequently, it is important to optimize the ejection speed, the height of falling, and the viscosity of solution when preparing cellulose beads through the dropping technique (Qi, 2011; Trygg et al., 2013).

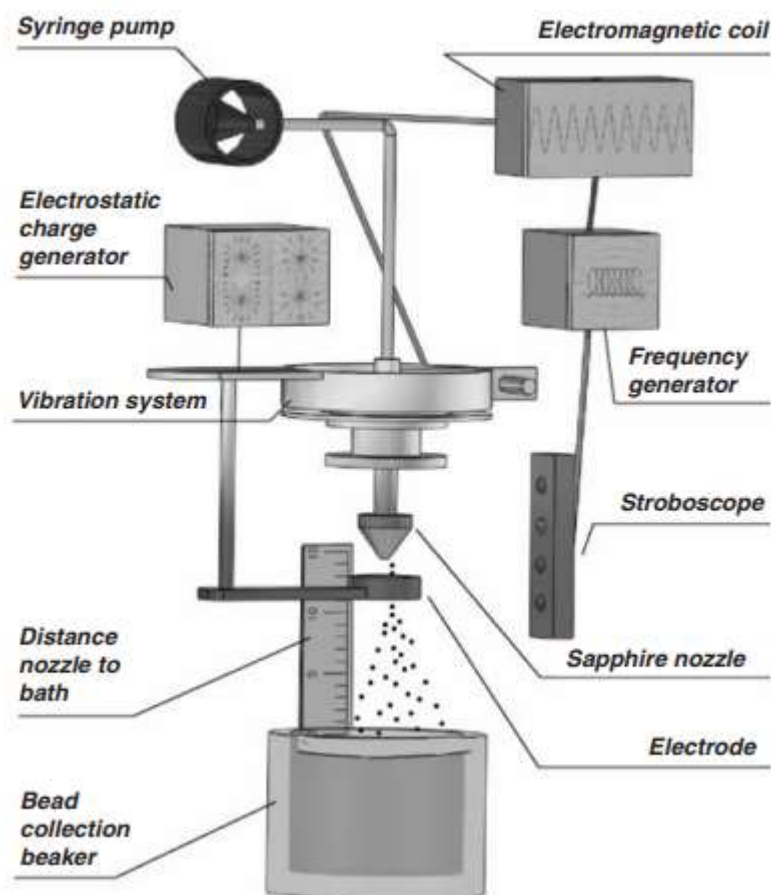


Figure 2.2 Schematic representation of dropping technology based on a vibrating nozzle (Mazzitelli et al., 2008).